THE JOURNAL OF PHYSICAL CHEMISTRY B

Article

pubs.acs.org/JPCB

Direct Characterization of Hydrophobic Hydration during Cold and Pressure Denaturation

Payel Das*[,†] and Silvina Matysiak*[,‡]

[†]Computational Biology Center, IBM Thomas J. Watson Research Center, Yorktown Heights, New York 10598, United States

[‡]Fischell Department of Bioengineering, University of Maryland, College Park, Maryland 20742, United States

Supporting Information

ABSTRACT: Cold and pressure denaturation are believed to have their molecular origin in hydrophobic interactions between nonpolar groups and water. However, the direct characterization of the temperature- and pressure-dependent variations of those interactions with atomistic simulations remains challenging. We investigated the role of solvent in the cold and pressure denaturation of a model hydrophobic 32-mer polymer by performing extensive coarse-grained molecular dynamics simulations including explicit solvation. Our simulations showed that the water-excluded folded state of this polymer is marginally stable and can be unfolded by heating or cooling, as well as by applying pressure, similar to globular proteins. We further detected essential population of a hairpin-like configuration prior to the collapse, which is consistently accompanied by a vapor bubble at the elbow of the kink. Increasing pressure suppresses formation of this vapor bubble by reducing water fluctuations in the hydration shell of the polymer, thus promoting unfolding. Further analysis revealed a slight reduction of water tetrahedrality in the polymer hydration shell compared to the bulk. Cold denaturation is driven by an enhanced tetrahedral ordering of hydration shell water than bulk water. At elevated pressures, the strikingly reduced fluctuations combined with the increase in interstitial water molecules in the polymer hydration shell contribute to weakening of hydrophobic interactions, thereby promoting pressure unfolding. These findings provide critical molecular insights into the changes in hydrophobic hydration during cold and pressure unfolding of a hydrophobic polymer, which is strongly related to the cold and pressure denaturation of globular proteins.

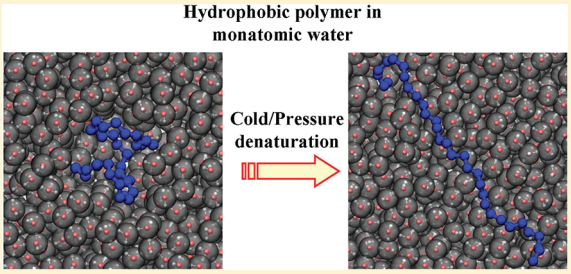

INTRODUCTION

Under physiological conditions, proteins adopt biologically active structures that are stable over a limited range of temperatures and pressures. The characteristic parabolic shape of the pressure−temperature stability diagram found for many globular proteins suggests heat-, cold-, and pressure-induced denaturation.[1] The stability of the native state is a result of several forces, including hydrogen bonds, electrostatics, and hydrophobic interactions. The subtle change in the relative strength of these interactions lies in the heart of protein denaturation.[2,3] Experimental and theoretical evidence suggest that the formation of a well-packed hydrophobic core is central to the native state stability. The liquid hydrocarbon model of the protein core implies that the nonmonotonic temperature dependence of protein stability primarily originates from the hydrophobic hydration phenomenon, i.e., transfer of an apolar solute from its pure phase into water.[4] Cold denaturation is thought to proceed largely as a result of changes in the nature of interaction between water and nonpolar groups. As temperature is decreased, the free energy penalty of the entropically unfavorable interaction between water and hydrophobe becomes smaller, leading to an increased tendency for nonpolar group hydration.[3,5] The experimentally observed loss of tertiary interactions upon cold denaturation thus reflects a weakening of hydrophobic associations.[6] The same liquid hydrocarbon model has been simultaneously used to account for pressure effects on protein stability; however, the model needed to be inverted.[7] Pressure denaturation is essentially viewed as the transfer of water into a pure hydrophobic phase. Taken together, both cold- and pressure-induced unfolding of proteins have their molecular origins in weakening of water-mediated hydrophobic interactions due to change in water structure. Thus, obtaining a microscopic picture of the cold and pressure denaturation phenomenon would facilitate understanding the driving forces in protein folding, in particular, the complex role played by the hydrophobic effect in the process.

Hydrophobic polymer collapse has long served as a paradigm for understanding protein (un)folding reactions. Recent theoretical work shows local water density depletion at the interface of hydrophobic polymers, leading to the formation of a transient, sufficiently large vapor bubble, which is the key event at the transition state of hydrophobic polymer collapse.[8,9] From this viewpoint, the tendency for a hydrophobic polymer to undergo drying-induced collapse will depend on water's proximity to its liquid−vapor coexistence. Thus, at both low temperatures and elevated pressures, the stability of the

Received: December 8, 2011
Revised: April 17, 2012
Published: April 18, 2012

   dx.doi.org/10.1021/jp211832c | J. Phys. Chem. B 2012, 116, 5342−5348

collapsed state will be reduced as water moves away from its phase equilibrium with vapor.

A study of protein/hydrophobic polymer stability using straightforward atomistic molecular simulations with explicit solvation is practically impossible due to the slow kinetics, resulting in insufficient conformational sampling at low temperatures and high pressures. For example, a fully atomistic MD simulation study of a hydrophobic polymer dissolved in a box of TIP5P water could not essentially explore the fully extended polymer within 100 ns of simulation time.[10] Because of the computational impasse, theoretical studies on cold/pressure denaturation are oftentimes based on lattice-based polymer and water models that can well describe the equilibrium properties but compromise in capturing crucial kinetic events, such as the bubble formation.[11−14] However, most off-lattice minimalist protein models renormalize the role of solvent through effective short-range inter-residue interactions.[15−20] In these models, the ground state is the protein's native state, which precludes the existence of a denatured state being more stable than the native state at lower temperatures. Thus, an implicit description is unlikely to account for cold, pressure, and thermal denaturation. Recently, Garde and coworkers have employed a water insertion method combined with atomistic molecular dynamics simulations to characterize the pressure-induced unfolded state of a protein system.[21,22] However, the straightforward and complete characterization of cold and pressure unfolding reactions remains unfeasible with existing models/methods. Such a study needs direct exploration of the variations in hydrophobic hydration over a range of pressures and temperatures.

We present a coarse-grained off-lattice homopolymer model combined with a monatomic water (mW) model[23] to fully explore the role of hydrophobicity during cold and pressure unfolding of a hydrophobic homopolymer. The proposed model has the potential to be extended to study folding and stability of real proteins by including chain stiffness through the definition of dihedral potentials. In this model, water is treated explicitly using the recently developed single particle mW water model that includes the tetrahedral hydrogen-bonding network in terms of three-body interactions. Although the potential energy terms do not include any electrostatic interactions and are short-range in nature, this coarse-grained water model precisely reproduces the structure, thermodynamics, anomalies, and whole phase diagram of water.[23] In addition, simulations with the mW model are ∼100 times faster than with atomistic water models with Ewald sums.

In this study, we have developed coarse-grained monomer−monomer and monomer−water potentials that, when combined with the mW model for water, exhibit pressure, cold, and heat denaturation. Our polymer model is realistic, in the sense that it includes monomer−water interactions. We have analyzed the role of water structural changes in hydrophobic hydration over a range of pressures and temperatures, which provides a microscopic view of the cold and pressure unfolding of the hydrophobic polymer. We have also studied the effect of polymer wettability, by tuning the monomer−water interaction, on its cold and pressure unfolding. As the proposed model incorporates a realistic hydrophobic protein-like polymer model in conjunction with an explicit treatment of the water-mediated interactions, it opens the possibility for the development of a coarse-grained model of natural proteins in aqueous environment. Such a model will provide a useful tool to study the effect of environment on protein stability and function.

MODEL AND METHODS

We report MD simulations of a coarse-grained hydrophobic homopolymer model combined with the recently developed monatomic water (mW) model[23] over a range of temperatures and pressures. The mW model represents each water molecule by a single particle. The water molecules interact through very short-ranged potentials. Interactions between mW particles are modeled using a parametrized Stillinger−Weber (SW) potential that was obtained by fitting to experimental data, such as vaporization enthalpy, melting temperature, and water density at room temperature.[23] This water model reproduces important properties of water like the prediction of hexagonal ice as a stable crystal structure at room pressure and its melting point, the enthalpy of ice, the density of the liquid at 300 K, the maximum density of liquid, and the liquid−vapor tension. This model has been used in the past to explore ranges of temperatures between 220−560 K and pressures 1−3000 atm.[23−25] Table S1, Supporting Information shows the density of the solvent at the (T,P) conditions studied in this work. More structural information of the solvent at T = 800 K is available in Figure S1, Supporting Information. The energy function and the parameters used in this potential are described in ref 23. Briefly, the SW potential can be described as $v = v_2(r) + \lambda v_3(r,\theta)$, a combination of a pairwise term $v_2(r)$ and a three-body term $v_3(r,\theta)$. The three-body term is scaled by the parameter λ that determines the strength of the tetrahedral interaction. For mW waters, λ is set to 23.15 to reproduce the experimental data, and θ_0 = 109.47° to effectively model the hydrogen-bonding network of atomistic water.

The hydrophobic polymer studied here comprises a linear chain of 32 monomers in which each monomer is presented with a single bead that has a mass equal to carbon. Each bead is covalently bonded to its nearest neighbor by a harmonic potential, $V_b = K_b(r - r_0)^2$ with a force constant K_b = 200 kcal/Å^2/mol and an equilibrium bond length r_0 = 1.53 Å (similar to the CH_2-CH_2 bond length). The two adjacent bonds are connected using a harmonic angle potential $V_a = K_a(\theta - \theta)$, with K_a = 12.12 kcal/deg/mol and θ_0 = 111° (similar to a $CH_2-CH_2-CH_2$ angle). The nonbonded pairwise interaction between monomers are modeled using a 9−6 form of a truncated Lennard-Jones (LJ) potential, such as $V_{nb} = 4\varepsilon_{mm}[(\sigma/r)^9 - (\sigma/r)^6]$, with a cutoff distance r_c = 8 Å. The pairwise monomer−monomer interaction strength ε_{mm} equals 0.35 kcal/mol. The polymer model is similar to what used in ref 26: in present study, the bead size is somewhere between methane and ethane like monomer with significantly stronger monomer−monomer interaction. The size of an individual monomer is set to 4 Å, and σ_{mw} is set to 3.2 Å. Nonbonded interactions between a monomer and its first and second nearest bonded neighbors, as well as dihedral interaction terms, are excluded to allow the investigation of conformational transitions of flexible hydrophobic polymers driven by hydrophobic interactions and their dependence on temperature and pressure.

Modeling real hydrophobic polymers requires consideration of monomer−water interactions because of ubiquitous van der Waals forces. Hence, we have modeled the monomer−water interactions using a potential energy function $V_{mw} = 4\varepsilon_{mw}[(\sigma/r)^9 - (\sigma/r)^6]$, similar to that used for the monomer−monomer interactions. The 9−6 form of the LJ potential has been used by others to model monomer−monomer and monomer−water interactions in a coarse-grained model of alkane chains in water.[27] We performed three

dx.doi.org/10.1021/jp211832c | J. Phys. Chem. B 2012, 116, 5342−5348

different sets of simulations with monomer−water interaction strength, ε_{mw}, equal to 0.325, 0.35, and 0.375 kcal/mol (while keeping the ε_{mm} unchanged, σ_{mw} is set to 3.2 Å) to explore the effect of water affinity of the polymer on its collapse transition.

The polymer was immersed in a cubic box containing 1021 mW waters. All simulations were performed using velocity verlet algorithm implemented in LAMMPS, a massively parallel MD software developed by Plimpton et al.[28] Use of this coarse-grained model allowed us to use a time step of 8 fs. All systems were equilibrated first in an NVT ensemble for 14 ps. Periodic boundary conditions were employed for all systems. All production runs were performed in an NPT ensemble using a Nose−Hoover thermostat and barostat with damping constants of 0.8 and 8 ps, respectively. For each system at a particular temperature and pressure, two different simulations were performed using the collapsed and the extended state of the polymer as the starting configuration, with a total simulation length of ∼320 ns.

RESULTS AND DISCUSSION

Hydrophobic Collapse of the Coarse-Grained Polymer Chain in mW Water. We first present the results characterizing the role of hydrophobic hydration in determining the conformational flexibility of the CG polymer chain, for which the monomer−monomer and the monomer−water interaction strengths are exactly same, i.e., $\varepsilon_{mm} = \varepsilon_{mw} = 0.35$ kcal/mol. Preliminary simulations showed that this polymer populates a stable collapsed state at $T = 400$ K and $P = 1$ atm (see Figure S2, Supporting Information). Figure 1a shows the two-dimensional potential of mean force (PMF) of this collapse transition as a function of radius of gyration of the polymer (r_g) and number of water−monomer contacts (n_{wm}) at 400 K and 1 atm. Here, a monomer−water contact is considered if an mW particle is within 5.45 Å of a monomer. At 400 K and 1 atm, the PMF reveals two basins corresponding to a collapsed state and an extended state (Figure 1a). The collapsed state shows a very compact helical (folded) conformation with an r_g of ∼4.3 Å, which is clearly more populated than the extended state (r_g ∼10 Å). The folded state is much less hydrated than the extended state, as suggested from the comparison of the number of monomer−water contacts formed in those two states, confirming the correct emergence of hydrophobic collapse of the polymer in mW water. This finding is in accordance with the previously proposed mechanism of entropically driven hydrophobic hydration phenomenon in which the polymer collapses by minimizing the solvent exposed surface area of its hydrophobic monomers, thereby limiting the number of interfacial water molecules to pay an entropic penalty for hydrogen bonding.[11] Upon increasing temperature, the polymer unfolds as the thermal energy compensates for this entropic penalty to form interfacial hydrogen bonds around exposed monomers (see Figure S3, Supporting Information). The formation of the water-excluded, folded state at 400 K and 1 atm essentially follows population of a slightly bent, otherwise extended, polymer configuration (see Figures 1a and S2, Supporting Information). This hairpin-like conformation with r_g values ∼5.5 Å is strikingly similar to the transition state structure proposed by Miller et al. for a hydrophobic polymer collapse reaction.[8] However, the ensemble of these slightly bent configurations does not appear to be well separated from the collapsed state ensemble by a distinct free-energy barrier, rather seems like a gradual transition, which is likely related to the choice of reaction coordinates. In fact, Miller et al. proposed that the free energy barrier separating the transition state from the collapsed state can be effectively captured by using the solvent coordinates, not the polymer chain coordinates.[8] The evaporation of water in the vicinity of the polymer provides the driving force for hydrophobic collapse.[9] Interestingly, the hairpin-like conformation was not populated in simulations in vacuum (no explicit mW particles); in that case the collapse is solely driven by monomer−monomer attractions.

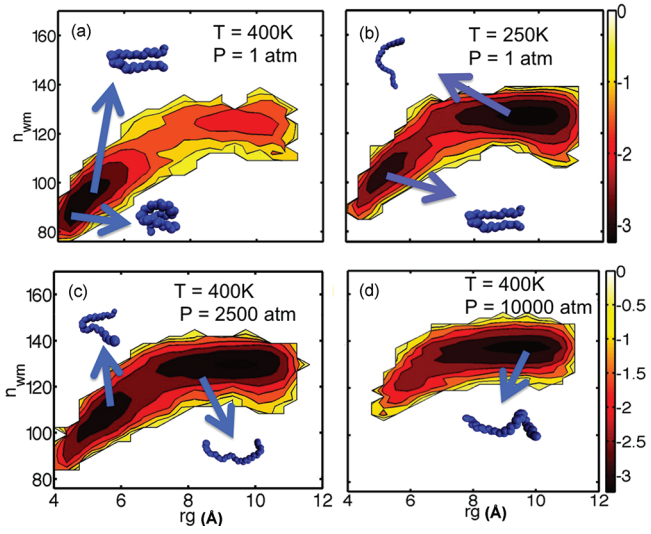

Figure 1. (a−d) Potential of mean force plots of the hydrophobic homopolymer in mW water, as a function of two reaction coordinates n_{wm} (number of water−monomer contacts) and r_g (radius of gyration). Each contour level marks a free energy change of 1 kcal/mol. Representative polymer conformations are shown.

Cold and Pressure Unfolding of the Polymer in mW Water. Given that our CG polymer model in mW water correctly exhibits hydrophobic collapse, we explored the temperature and pressure dependence of this collapse transition (Figures 1 and S2, Supporting Information). As the temperature is lowered to 250 K (keeping the pressure fixed at 1 atm), the PMF (Figure 1b) reveals higher probability of exploring the fully extended polymer configurations, suggesting cold denaturation. Experimental evidence suggests that the cold-denatured state is more compact than the heat-unfolded state for proteins and resembles a compact swollen conformation with significant retention of secondary structure.[6,29−31] It is likely that, due to the use of a relatively short (compared to proteins) homopolymer, here a complete unfolding is observed at low temperatures. Furthermore, the polymer at this low temperature infrequently visits the compact folded state. The shift in the location of the free energy minimum corresponding to the structures with low radius of gyration suggests higher occurrence of the hairpin-like polymer configurations that are better hydrated.

At intermediate pressure ($P = 2500$ atm and $T = 400$ K), the PMF profile exhibits a single transition between the fully extended and the hairpin-like states (Figure 1c). The fact that the 'pressure folded state' has a hairpin-like structure, instead of a collapse helical one, is a clear indication that the hydrophobic collapse is reduced in those situations. This observation is in line with the experimentally reported loss of protein structure (mainly quaternary and tertiary) at intermediate pressures ($P <$ 3000 atm).[32−35] It is worth mentioning that the pressure-

dx.doi.org/10.1021/jp211832c | J. Phys. Chem. B 2012, 116, 5342−5348

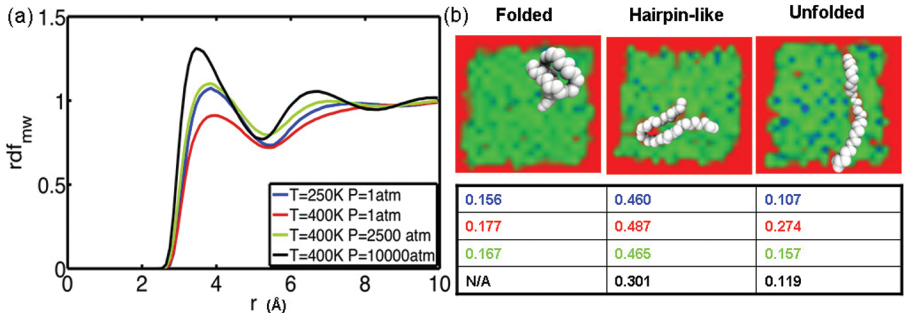

Figure 2. (a) Monomer–water radial distribution functions computed using all polymer conformations for a range of temperatures and pressures. (b) Water density map and fluctuations in the hydration shell for the folded, hairpin, and unfolded conformations at T = 400 K and P = 1 atm. The water number density (red to blue: low to high) was computed by additively distributing normalized Gaussians of width equal to atomic radius of mW particle (i.e., oxygen atom) on a 2 Å grid. Water density fluctuations in the hydration shell for folded, hairpin, and unfolded conformations are tabulated at the bottom. The colors of the text correspond to the different pressures and are the same as those used in the left panel. At P = 10 000 atm, there is not significant population of helical conformations to compute the water fluctuations.

induced hairpin-like state is slightly more hydrated than the cold-induced hairpin-like state. The fact that the pressure folded state has a hairpin-like structure, instead of a collapse helical one, is a clear indication that the hydrophobic collapse is reduced in those situations. At very high pressure (P = 10 000 atm and T = 400 K), the polymer exclusively populates the fully extended state during the simulation time of 320 ns (Figure 1d). Interestingly, it has been observed experimentally that complete loss of secondary structure in several proteins occurs at pressures above 5000 atm.[32,35,36] The unfolded polymer conformation at high pressure (P = 10 000 atm) appears to be slightly more hydrated than the one observed at an intermediate pressure (P = 2500 atm), as indicated by the number of water–monomer contacts formed with the unfolded state. Taken together, our simulations of a coarse-grained hydrophobic polymer immersed in mW waters allow complete exploration of the cold and pressure unfolding reactions within a reasonable simulation time (few hundred nanoseconds).

Weakening of Hydrophobic Interactions at Cold Temperatures and Elevated Pressures. Figure 2a shows the monomer–water radial distribution function (rdf_{mw}) ensemble averaged over all polymer configurations. At T = 400 K and P = 1 atm (under the conditions at which the polymer remains mostly collapsed), the rdf_{mw} shows a first minimum at 5.45 Å, suggesting the existence of a hydration shell for the polymer (Figure 2a), which is very close to the width of the hydrocarbon–water interface.[27] The polymer becomes better hydrated at both cold T and high P, suggesting a weakening of hydrophobic interactions, as indicated by an increase in the height of the first peak. Lowering T does not modify the location of the first peak and the minimum. On the contrary, an increase in pressure causes the first peak and the minimum to shift toward lower distances. At higher pressure (10 000 atm), the polymer–water rdf becomes more defined with emergence of a second peak at ~6.5 Å, consistent with the pressure response of hydration shell waters of hydrophobic solutes observed by Garde and co-workers.[21] Moreover, pressure compresses the hydration shell of the polymer, as evident from a shift of the first minimum to a lower distance. Similar results are obtained from rdf_{mw} computed using only the folded conformations as well (see Figure S4, Supporting Information).

To further investigate the role of water on the pressure dependence of the collapse mechanism, we have computed the normalized water fluctuations $[\langle N^2\rangle - \langle N^2\rangle]/\langle N\rangle$ for the folded, unfolded, and the hairpin-like conformations at different temperatures and pressures (Figure 2b). Recently, Garde and co-workers suggested pressure-induced suppression of water fluctuations in the first hydration shell of proteins.[21] They have further demonstrated that water fluctuation of the unfolded state with larger exposure of hydrophobic residues is higher than that of the folded state. In accordance with that, we find that the normalized water fluctuation in the hydration shell of the unfolded state is 0.277, higher than that of the folded state (0.174) at 400 K and 1 atm. However, the difference in water fluctuations between folded and unfolded states is reduced with increasing pressure (see Figure 2b), consistent with previous observations suggesting pressure-induced weakening of hydrophobicity leading to unfolding.[21]

Interestingly, the hairpin-like structure experiences much larger water fluctuation compared to both folded and unfolded states at 400 K and 1 atm. For example, at 400 K and 1 atm, the normalized water fluctuation in the hydration shell of the hairpin-like conformation is 0.487, significantly higher than those reported for the folded and unfolded conformations. As depicted in Figure 2b, a local depletion in water density is observed in the elbow of the kink of the hairpin-like conformation, leading to a vapor bubble formation. This finding is in agreement with the previous work by Chandler and co-workers, suggesting the bubble formation as the major rate-limiting step of hydrophobic polymer collapse.[8] This dewetting event[37] is analogous to the large length-scale water density fluctuations observed between hydrophobic plates[38] or multimeric protein complexes.[39] Thus, enhanced fluctuations of the hydration shell water molecules coupled with a vapor bubble formation near the kink characterize this hairpin-like transition state conformation. Interestingly, the fluctuations are slightly reduced from 0.487 to 0.465 for the hairpin-like conformation while increasing the pressure from 1 to 2500 atm. With further increase of the pressure to 10 000 atm, the fluctuations are strikingly lowered to 0.301, implying that the free-energy barrier associated with a critical size vapor bubble formation becomes higher with increasing pressure. As a result, a critical size vapor bubble is rarely visited at 10 000 atm (see Figure S5, Supporting Information), making the hydrophobic collapse kinetically unfavorable.

Alteration in Water Structure Induces Cold and Pressure Unfolding. To directly characterize the role of hydrophobic interactions in the denaturation process, we have analyzed the solvent structural changes with temperature and

dx.doi.org/10.1021/jp211832c | J. Phys. Chem. B 2012, 116, 5342–5348

pressure. For this purpose, we computed two functions: the water−water radial distribution function (rdf_{ww}) and the O−O−O triple angle distribution function (adf). These radial and angular distributions are widely used in neutron[40] and X-ray diffraction[41,42] experiments to characterize the structure of liquid water. The coarse-grained water models with isotropic potentials[43] are known to reproduce the rdf_{ww} but not the adf. The introduction of anisotropic interactions by the use of a three-body interaction term in the potential allows the mW water model to reproduce both rdf_{ww} and adf functions.[23]

As shown in Figure 3, at cold temperature, the two typical maxima of the rdf_{ww} (one at 2.8 Å and one at 4.5 Å)

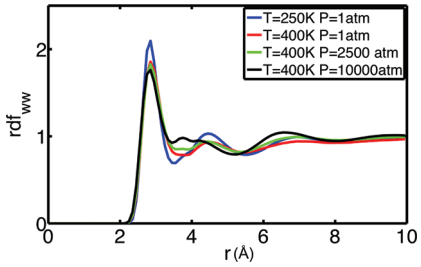

Figure 3. Hydration shell water−water radial distribution functions for a range of temperatures and pressures.

corresponding to the two coordinating spheres around a reference water molecule becomes higher and more defined, indicating stronger tetrahedral ordering of hydration shell water molecules. However, a peak at 3.8 Å emerges in the rdf_{ww} at the expense of the one at 4.5 Å at higher pressures, suggesting the presence of interstitial water molecules that is consistent with previous experimental[40] and theory/simulation data.[44] Interstitial water molecules are second-shell neighbors; however, they are closer to the central water molecule than other second-shell neighbors. Presence of interstitial water molecules occurs as a result of pressure-induced collapse of the second coordination shell onto the first one, which is clear from the somewhat arbitrary location of the first minimum at very high pressures (10 000 atm). However, the number of hydrogen bonds for a central water molecule does not change substantially with pressure (little change in the 2.8 Å structure), implying no major deformation of the tetrahedral first coordination shell, consistent with neutron scattering data.[40]

Deeper insights onto the changes in water orientational structure can be obtained from the adf. The ∠O1−O−O1 adf provides structural information for the first coordination shell waters (Figure S6, Supporting Information). In this case, the four closest water molecules are considered as the constituents of the first coordination shell and are labeled as O1. A second ∠O1−O−O2 adf was also computed involving the first (O1) and the 5th−8th neighbors of the second coordination shell waters (O2) [Figure 4]. The subshell comprising the 5th−8th neighbors from the second coordination shell is reported to undergo pressure-induced change in literature.[40,45] At ambient conditions (400 K and 1 atm), the ∠O1−O−O1 adfs for both hydration shell and bulk water molecules show a single characteristic peak at ∼109°, confirming the tetrahedral nature of water (Figure S6, Supporting Information). The distributions for the hydration shell and bulk water molecules match well at all temperatures and pressures, implying no deformation of the tetrahedral structure in the first coordination shell near the polymer (Figure S6, Supporting Information).

With lowering temperature, the water molecules become more tetrahedrally ordered (as the peaks become narrower). The ∠O1−O−O1 adf is moderately affected with pressure, with the distribution peak shifted toward slightly lower angles. This observation does not imply loss of tetrahedrality, rather a mere consequence of significant overlap of the first and second coordination shells, which is obvious from the ∠O1−O−O2 adf (Figure 4). In this adf, two peaks at 50° and at 80° are evident for bulk water at ambient conditions. The first peak belongs to the 5−8 subshell of the second-shell water molecules

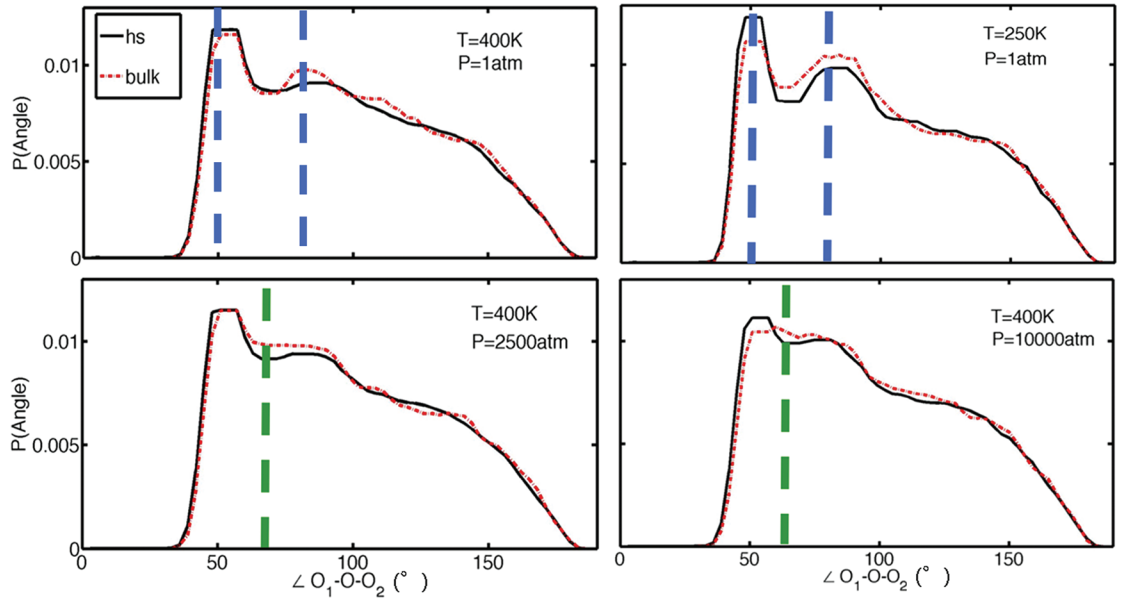

Figure 4. Angular distribution ($\angle O_1-O-O_2$) between the first and second nearest neighbor water molecules at different temperatures and pressures. First neighbors are considered to be the 1st−4th and second neighbors are the 5th−8th nearest neighbors of a reference water molecule. The effect of increasing pressure is evident in the apparent merging of the two peaks at 50° and at 80° (shown in blue lines) into a single one. The green line denotes the angle around 65° that is due to interstitial water molecules. At low temperatures, the peaks that correspond to 50° and 80° are enhanced.

dx.doi.org/10.1021/jp211832c | J. Phys. Chem. B 2012, 116, 5342−5348

that are forming tetrahedral angles with one of the first shell neighbors, $O1^{i}$. The peak at 80° corresponds to those second-shell molecules that form tetrahedral angles with any of the other three first-shell neighbors $O1^{i\neq j}$ to the central molecule. The region between the two peaks with a ∠O1−O−O2 angle of ∼65° represents the interstitial water molecules.[45] At ambient conditions, the hydration shell water molecules appear to be slightly less tetrahedral than the bulk water, as the second peak around 80° is lower. This finding implies that the presence of a nonpolar solute locally perturbs the orientational structure of not the first but the second coordination shell of water. This observation is consistent with Muller's modified hydration-shell hydrogen-bond model,[46] stating that "the hydrogen bonds in the hydration shell of nonpolar solutes are enthalpically stronger but *more* broken than those in bulk water,"[47] which has been validated using both experiments[48] and theory/simulations.[47,49]

The changes in hydrophobic hydration upon lowering the temperature are evident from ∠O1−O−O2 angle distribution. The hydration shell water becomes more tetrahedrally ordered than bulk water at 250 K, as the two peaks become narrower, higher, and better defined. In addition, the minimum around 65° drops to a lower probability, implying a pronounced reduction of interstitial water molecules near the polymer. Taken together, increased hydration of the polymer and higher structural ordering of the hydration shell water suggest that unfolding at low temperature is driven by an enthalpic benefit associated with the formation of additional monomer−water contacts as well as stronger water−water contacts in the second coordination shell. Therefore, lowering the entropy of the system by cooling allows forming more monomer−water contacts as well as stronger tetrahedral interactions for interfacial waters, which were restricted at ambient conditions. These results indicate possible heat release from the hydration shell of the hydrophobic polymer immersed in cold water, which is in agreement with the experimentally observed behavior of cold-denaturation of proteins.[50]

However, the marked probability enhancement of the ∠O1−O−O2 angles around 65° unambiguously reveals the pressure-induced collapse of the second coordination shell into the first one, and the resulting increase in interstitial water molecules, for both bulk and hydration shell water, is consistent with previous studies.[45] The two peaks completely merge into a single one at 10 000 atm for bulk water. Interestingly, the interstitial water molecules are less probable in the hydrophobic hydration shell than in bulk water even at elevated pressures such as 10 000 atm, suggesting the pressure-induced collapse of the second coordination shell is less intense in the hydration shell. Nevertheless, a significant enhancement in the probability of interstitial water molecules as well as dramatically reduced water fluctuations is noticed near the polymer at elevated pressure. Such changes in water structure and fluctuations contribute to the reduction of hydrophobic interactions between polymer and water at increased pressure.

How Do Polymer−Water Attractions Affect Cold and Pressure Denaturation? To answer this question, we studied cold and pressure denaturation of the polymer with different monomer−water affinities; (i) with a reduced ε_{mw} of 0.325 kcal/mol and (ii) with a larger ε_{mw} of 0.375 kcal/mol (see model and methods section and Figure S7, Supporting Information). In agreement with Athawale et al.,[26] a larger ε_{mw} triggers a less pronounced collapse at ambient conditions, as the interfacial water molecules benefit from energetic gain through stronger monomer−water interactions.[26,30] This energetic bonus also plays a role at the cold temperatures and high pressures, as the increase in polymer−water attractions favors denaturation. However, at very high pressure such as 10 000 atm, the denaturation seems to be independent of polymer−water attractions.

CONCLUSIONS

We investigated the role of solvent in the cold and pressure denaturation of a model hydrophobic 32-mer polymer by performing extensive coarse-grained molecular dynamics simulations including explicit solvation. Our simulations showed that the water-excluded folded state of this polymer is marginally stable (at 400 K and 1 atm), when the strengths of monomer−water dispersive interactions and monomer−monomer dispersive interactions are equal. The stability of this folded state was found to be analogous to globular proteins, as the model polymer can be unfolded by heating or cooling, as well as by applying pressure. We further detected essential population of a hairpin-like configuration prior to the collapse, which is consistently accompanied by a vapor bubble at the elbow of the kink. Similar observation has been reported before.[8] Increasing pressure suppresses formation of this vapor bubble by reducing water fluctuations in the hydration shell of the polymer, thus promoting unfolding.

To further characterize the role of hydrophobic interactions in cold and pressure unfolding, the water structure was thoroughly analyzed. At ambient temperature and pressure, a slight reduction in water tetrahedrality was revealed in the hydration shell compared to bulk, consistent with Muller's modified hydration-shell hydrogen-bond model.[46] With lowering temperature, the hydration shell water was found to be more tetrahedral than bulk water. This observation clearly implies that, at low temperatures, the water molecules in the hydration shell exist in a lower energy state, thus explaining the heat release during cold denaturation as opposed to heat adsorption during thermal denaturation. However, a pressure-induced collapse of the second coordination shell into the first one was detected for both hydration shell and bulk water. The strikingly reduced fluctuations combined with the presence of interstitial water molecules in the hydration shell contribute to weakening of hydrophobic interactions between the polymer and pressurized water, thereby promoting pressure unfolding.

In conclusion, this coarse-grained simulation study provides a mechanistic understanding of the molecular changes in hydrophobic hydration during cold and pressure unfolding of a model hydrophobic polymer, which is also important in the context of realistic biological self-assembly processes, such as protein folding. The relative contribution of monomer−monomer interaction, monomer−water interaction, and hydrophobicity in determining polymer stability at various T and P needs to be further investigated in a quantitative manner, which will be addressed in the future. We believe that the coarse-grained model presented in this article provides a solid starting point for developing novel theoretical methods aimed at a direct characterization of the role of water in protein folding, dynamics, and function.

ASSOCIATED CONTENT

Supporting Information

Additional figures on cold and pressure unfolding of hydrophobic polymer in mW water. This material is available free of charge via the Internet at http://pubs.acs.org.

dx.doi.org/10.1021/jp211832c | J. Phys. Chem. B 2012, 116, 5342−5348

AUTHOR INFORMATION

Corresponding Author

*E-mail: daspa@us.ibm.com (P.D.); matysiak@umd.edu (S.M.).

Notes

The authors declare no competing financial interest.

ACKNOWLEDGMENTS

We are indebted to Hernan Stamati for his suggestions and assistance with computer-related problems. This research was supported in part by the National Science Foundation through TeraGrid resources provided by The Texas Advanced Computing Center (TACC) under grant number [TG-MCB110075]. P.D. would like to thank the IBM BlueGene Science program for the support. We also thank Ruhong Zhou and Bruce Berne for useful discussions.

REFERENCES

(1) Ravindra, R.; Winter, R. *ChemPhysChem* **2003**, *4* (4), 359−65.
(2) Hawley, S. A. *Biochemistry* **1971**, *10* (13), 2436−42.
(3) Privalov, P. L. *Crit. Rev. Biochem. Mol. Biol.* **1990**, *25* (4), 281−305.
(4) Kauzmann, W. *Nature* **1987**, *325* (6107), 763.
(5) Lopez, C. F.; Darst, R. K.; Rossky, P. J. *J. Phys. Chem. B* **2008**, *112* (19), 5961−7.
(6) Davidovic, M.; Mattea, C.; Qvist, J.; Halle, B. *J. Am. Chem. Soc.* **2009**, *131* (3), 1025−36.
(7) Hummer, G.; Garde, S.; Garcia, A. E.; Paulaitis, M. E.; Pratt, L. R. *Proc. Natl. Acad. Sci. U.S.A.* **1998**, *95* (4), 1552−5.
(8) Miller, T. F.; Vanden-Eijnden, E.; Chandler, D. *Proc. Natl. Acad. Sci. U.S.A.* **2007**, *104* (37), 14559−14564.
(9) ten Wolde, P. R.; Chandler, D. *Proc. Natl. Acad. Sci. U.S.A.* **2002**, *99* (10), 6539−6543.
(10) Paschek, D.; Nonn, S.; Geiger, A. *Phys. Chem. Chem. Phys.* **2005**, *7* (14), 2780−2786.
(11) Patel, B. A.; Debenedetti, P. G.; Stillinger, F. H.; Rossky, P. J. *Biophys. J.* **2007**, *93* (12), 4116−4127.
(12) De Los Rios, P.; Caldarelli, G. *Phys. Rev. E* **2000**, *62* (6 Pt B), 8449−52.
(13) Buldyrev, S. V.; Kumar, P.; Debenedetti, P. G.; Rossky, P. J.; Stanley, H. E. *Proc. Natl. Acad. Sci. U.S.A.* **2007**, *104* (51), 20177−20182.
(14) Xu, L.; Buldyrev, S. V.; Angell, C. A.; Stanley, H. E. *Phys. Rev. E* **2006**, *74* (3), 031108.
(15) Das, P.; Wilson, C. J.; Fossati, G.; Wittung-Stafshede, P.; Matthews, K. S.; Clementi, C. *Proc. Natl. Acad. Sci. U.S.A.* **2005**, *102* (41), 14569−14574.
(16) Head-Gordon, T.; Brown, S. *Curr. Opin. Struct. Biol.* **2003**, *13* (2), 160−167.
(17) Das, P.; Matysiak, S.; Clementi, C. *Proc. Natl. Acad. Sci. U.S.A.* **2005**, *102* (29), 10141−10146.
(18) Matysiak, S.; Clementi, C. *J. Mol. Biol.* **2004**, *343* (1), 235−248.
(19) Pincus, D. L.; Cho, S. S.; Hyeon, C.; Thirumalai, D.; Conn, P. M. Minimal Models for Proteins and RNA: From Folding to Function. In *Progress in Molecular Biology and Translational Science*; Academic Press: New York, 2008; Vol. *84*, Chapter 6, pp 203−250.
(20) Onuchic, J. N.; Luthey-Schulten, Z.; Wolynes, P. G. *Annu. Rev. Phys. Chem.* **1997**, *48*, 545−600.
(21) Sarupria, S.; Garde, S. *Phys. Rev. Lett.* **2009**, *103* (3), 037803.
(22) Sarupria, S.; Ghosh, T.; Garcia, A. E.; Garde, S. *Proteins* **2010**, *78* (7), 1641−51.
(23) Molinero, V.; Moore, E. B. *J. Phys. Chem. B* **2009**, *113* (13), 4008−16.
(24) DeMille, R. C.; Cheatham, T. E., III; Molinero, V. *J. Phys. Chem. B* **2011**, *115* (1), 132−42.
(25) Limmer, D. T.; Chandler, D. *J. Chem. Phys.* **2011**, *135* (13), 134503.
(26) Athawale, M. V.; Goel, G.; Ghosh, T.; Truskett, T. M.; Garde, S. *Proc. Natl. Acad. Sci. U.S.A.* **2007**, *104* (3), 733−738.
(27) Shelley, J. C.; Shelley, M. Y.; Reeder, R. C.; Bandyopadhyay, S.; Klein, M. L. *J. Phys. Chem. B* **2001**, *105* (19), 4464−4470.
(28) Plimpton, S. *J. Comput. Phys.* **1995**, *117*, 1−19.
(29) Babu, C. R.; Hilser, V. J.; Wand, A. J. *Nat. Struct. Mol. Biol.* **2004**, *11* (4), 352−7.
(30) Hallerbach, B.; Hinz, H. J. *Biophys. Chem.* **1999**, *76* (3), 219−27.
(31) Yang, W. Y.; Gruebele, M. *Philos. Trans. R. Soc., A* **2005**, *363* (1827), 565−73.
(32) Paliwal, A.; Asthagiri, D.; Bossev, D. P.; Paulaitis, M. E. *Biophys. J.* **2004**, *87* (5), 3479−92.
(33) Smeller, L.; Meersman, F.; Heremans, K. *Biochim. Biophys. Acta* **2006**, *1764* (3), 497−505.
(34) Oliveira, A. C.; Gaspar, L. P.; Da Poian, A. T.; Silva, J. L. *J. Mol. Biol.* **1994**, *240* (3), 184−7.
(35) Woenckhaus, J.; Kohling, R.; Thiyagarajan, P.; Littrell, K. C.; Seifert, S.; Royer, C. A.; Winter, R. *Biophys. J.* **2001**, *80* (3), 1518−23.
(36) Webb, J. N.; Webb, S. D.; Cleland, J. L.; Carpenter, J. F.; Randolph, T. W. *Proc. Natl. Acad. Sci. U.S.A.* **2001**, *98* (13), 7259−64.
(37) Berne, B. J.; Weeks, J. D.; Zhou, R. *Annu. Rev. Phys. Chem.* **2009**, *60* (1), 85−103.
(38) Huang, X.; Margulis, C. J.; Berne, B. J. *Proc. Natl. Acad. Sci. U.S.A.* **2003**, *100* (21), 11953−11958.
(39) Zhou, R.; Huang, X.; Margulis, C. J.; Berne, B. J. *Science* **2004**, *305* (5690), 1605−9.
(40) Strassle, T.; Saitta, A. M.; Godec, Y. L.; Hamel, G.; Klotz, S.; Loveday, J. S.; Nelmes, R. J. *Phys. Rev. Lett.* **2006**, *96* (6), 067801.
(41) Soper, A. K. *J. Phys.: Condens. Matter* **2007**, *19* (33), 335206.
(42) Narten, A. H.; Levy, H. A. *J. Chem. Phys.* **1971**, *55* (5), 2263−2269.
(43) Johnson, M. E.; Head-Gordon, T.; Louis, A. A. *J. Chem. Phys.* **2007**, *126* (14), 144509−10.
(44) Urquidi, J.; Singh, S.; Cho, C. H.; Robinson, G. W. *Phys. Rev. Lett.* **1999**, *83* (12), 2348.
(45) Saitta, A. M.; Datchi, F. D. R. *Phys. Rev. E* **2003**, *67* (2), 020201.
(46) Muller, N. *Acc. Chem. Res.* **1990**, *23* (1), 23−28.
(47) Graziano, G.; Lee, B. *J. Phys. Chem. B* **2005**, *109* (16), 8103−8107.
(48) Bowron, D. T.; Filipponi, A.; Roberts, M. A.; Finney, J. L. *Phys. Rev. Lett.* **1998**, *81* (19), 4164−4167.
(49) Laidig, K. E.; Daggett, V. *J. Phys. Chem.* **1996**, *100* (14), 5616−5619.
(50) Privalov, P. L.; Griko, Y. V.; Venyaminov, S. Y.; Kutyshenko, V. P. *J. Mol. Biol.* **1986**, *190* (3), 487−498.